HHS Public Access

Author manuscript

Sci Transl Med. Author manuscript; available in PMC 2020 April 06.

Published in final edited form as:

Sci Transl Med. 2019 July 03; 11(499): . doi:10.1126/scitranslmed.aau6627.

Retinol binding protein 3 is increased in the retina of patients with diabetes resistant to diabetic retinopathy

Hisashi Yokomizo[1,*], **Yasutaka Maeda**[1,*], **Kyoungmin Park**[1], **Allen C. Clermont**[1,2], **Sonia L. Hernandez**[1], **Ward Fickweiler**[1,2], **Qian Li**[1], **Chih-Hao Wang**[1], **Samantha M. Paniagua**[1], **Fabricio Simao**[1], **Atsushi Ishikado**[1], **Bei Sun**[1], **I-Hsien Wu**[1], **Sayaka Katagiri**[1], **David M. Pober**[1], **Liane J. Tinsley**[1], **Robert L. Avery**[3], **Edward P. Feener**[1,4], **Timothy S. Kern**[5], **Hillary A. Keenan**[1,4], **Lloyd Paul Aiello**[1,2,6], **Jennifer K. Sun**[1,2,6], **George L. King**[1,4,6,†]

[1]Research Division, Joslin Diabetes Center, Boston, MA 02215, USA

[2]Beetham Eye Institute, Joslin Diabetes Center, Boston, MA 02215, USA

[3]California Retina Consultants, Santa Barbara, CA 93103, USA

[4]Department of Medicine, Harvard Medical School, Boston, MA 02115, USA

[5]Center for Translational Vision Research, Gavin Herbert Eye Institute, Irvine, CA 92697, USA

[6]Department of Ophthalmology, Harvard Medical School, Boston, MA 02114, USA

Abstract

The Joslin Medalist Study characterized people affected with type 1 diabetes for 50 years or longer. More than 35% of these individuals exhibit no to mild diabetic retinopathy (DR), independent of glycemic control, suggesting the presence of endogenous protective factors against DR in a subpopulation of patients. Proteomic analysis of retina and vitreous identified retinol binding protein 3 (RBP3), a retinol transport protein secreted mainly by the photoreceptors, as elevated in Medalist patients protected from advanced DR. Mass spectrometry and protein expression analysis identified an inverse association between vitreous RBP3 concentration and DR severity. Intravitreal injection and photoreceptor-specific overexpression of RBP3 in rodents inhibited the detrimental effects of vascular endothelial growth factor (VEGF). Mechanistically, our results showed that recombinant RBP3 exerted the therapeutic effects by binding and inhibiting VEGF receptor tyrosine phosphorylation. In addition, by binding to glucose transporter 1 (GLUT1) and decreasing glucose uptake, RBP3 blocked the detrimental effects of hyperglycemia in inducing inflammatory cytokines in retinal endothelial and Müller cells.

[†]Corresponding author. george.king@joslin.harvard.edu.
[*]These authors contributed equally to this work.

Author contributions: G.L.K. conceived the project, designed the experiments, and wrote and reviewed the manuscript. H.Y. and Y.M. wrote the drafts of the manuscript and performed most of the experiments. K.P., A.C.C., S.L.H., W.F., Q.L., C.-H.W., F.S., A.I., B.S., and S.K. performed some of the in vitro and in vivo experiments. S.M.P., I.-H.W., D.M.P., and L.J.T. assisted with data analysis. E.P.F. assisted with the proteomic experiments. T.S.K. performed retinal pathology experiments. R.L.A., L.P.A., and J.K.S. assisted with obtaining human retina and vitreous. K.P., H.A.K., L.P.A., and J.K.S. participated in the design of the experiments and editing the manuscript.

Competing interests: The authors declare that they have no competing interests.

Data and materials availability: All data underlying the findings reported in this manuscript are provided as part of the article. The proteomics data reported in this paper are provided in the Supplementary Materials, and the complete lists of peptide hits are included in tables S5 and S6.

Elevated expression of photoreceptor-secreted RBP3 may have a role in protection against the progression of DR due to hyperglycemia by inhibiting glucose uptake via GLUT1 and decreasing the expression of inflammatory cytokines and VEGF.

INTRODUCTION

Diabetic retinopathy (DR) affects most of the people with diabetes lasting longer than 20 years and is a leading cause of vision loss in developed countries (1, 2). Multiple mechanisms related to the toxic effects of hyperglycemia on the retina have been proposed to underlie the initiation and progression of DR (3). For example, elevated vascular endothelial growth factor (VEGF) expression in the retina plays a causal role in development of proliferative DR (PDR), and anti-VEGF agents are effective therapies for PDR and diabetic macular edema (4, 5). However, clinical trials targeting the adverse effects of hyperglycemia have not proven to delay or prevent the progression of non-PDR (NPDR) (6).

Recent epidemiological reports on factors that contribute to the development of diabetic (DM) complications have indicated that endogenous protective factors could be as important as risk factors (7). Studies of the Joslin 50-year Medalist cohort, composed of individuals who have had insulin-dependent diabetes for 50 years or longer, strongly suggest that endogenous protective factors exist that neutralize the toxic effects of hyperglycemia. More than 35% of the Medalist cohort does not exhibit advanced retinopathy, nephropathy, or neuropathy despite glycemic control similar to those that develop these complications (8). DR severity in the Medalist cohort exhibits a bimodal distribution with a substantial proportion of individuals with either no-mild NPDR (35%) or PDR (50%) but only a small group of Medalist patients with moderate-severe NPDR (5%) (9, 10). The bimodal distribution of DR severity, and the lack of association with glycemic control, suggests that protective factors might exist in the retina that delay progression of DR.

To identify potential retinal protective factors, we assessed protein profiles of the retina and vitreous in cadaveric eyes from patients in the Medalist cohort with no-mild NPDR by mass spectrometry and compared to those with documented PDR. Candidate secretory proteins that were found to be elevated in both the retina and the vitreous of the protected patients were selected for further cell and animal studies to test their capacity to prevent or ameliorate DR progression.

RESULTS

Characterization of proteins elevated in both the retina and vitreous

To identify potential protective factors against the development of PDR, we compared the retina and vitreous from patients in the Medalist cohort with no-mild NPDR ($n = 6$ eyes and $n = 4$ individuals) to those with PDR ($n = 11$ eyes and $n = 6$ individuals) using mass spectrometry [liquid chromatography–tandem mass spectrometry (LC-MS/MS)]. Clinical characteristics of the Medalist patients did not differ between groups (table S1). Proteomic analysis by LC-MS/MS showed that retinol binding protein 3 (RBP3) and three other proteins were elevated ($P < 0.05$) in both retina and vitreous (tables S2 and S3). Peptide

numbers of RBP3 were increased by 1.6-fold in the retina ($P = 0.04$) and by 1.9-fold in the vitreous ($P = 0.005$) of Medalist patients with no-mild NPDR compared to PDR (Fig. 1, A and B). RBP3 was selected for further analysis due to its unique presence in the neuroretina and to the fact that previous studies showed that its deficiency can cause neuroretinal degeneration (11–13). In addition, RBP3 has been reported to be decreased in DR (14).

Validation of elevated concentrations of RBP3 in protected eyes

Vitreous RBP3 concentrations were assessed further in a larger and more diverse cohort that included 33 Medalist patients (type 1 diabetes, $n = 33$) and 21 non-Medalist patients [type 1 diabetes, $n = 2$; type 2 diabetes, $n = 6$; nondiabetic (NDM) controls, $n = 13$] using a specific and highly sensitive enzyme-linked immunosorbent assay (ELISA) for RBP3 (table S4), which did not detect albumin, immunoglobulin G, or RBP4 (fig. S1A). Age at DM onset and DM duration was different between the DR groups, as expected, due to group differences in diabetes type. Other clinical characteristics including hemoglobin A1c (HbA1c) did not change substantially between DR groups (HbA1c, 7.0 to 7.4% from NPDR to PDR groups). Median vitreous RBP3 concentrations measured by ELISA in individuals with no-mild NPDR, moderate NPDR, and PDR were 2.20 μg/ml (16.3 nM, $P < 0.05$), 1.91 μg/ml (14.1 nM, $P < 0.05$), and 0.95 μg/ml (7.1 nM, $P < 0.01$), respectively, and were decreased compared to the NDM group, 5.42 μg/ml (40.1 nM; Fig. 1C). Vitreous RBP3 concentration was not correlated with HbA1c ($P = 0.83$; fig. S9) (9, 15). Vitreous VEGF concentration in the same cohort demonstrated gradual elevation with increasing severity of DR ($P < 0.05$; Fig. 1D). The ratio of RBP3 to VEGF concentrations, a possible index of protective capacity, steadily declined from NDM to no-mild NPDR, moderate NPDR, and PDR ($P < 0.01$ to $P < 0.0001$; Fig. 1E). Vitreous interleukin-6 (IL-6) concentrations were elevated in people with PDR compared to no-mild NPDR (fig. S1B).

Effects of diabetes and retinopathy on molecular sizes of vitreous RBP3

Immunoblot analysis with a polyclonal antibody made against human RBP3 (hRBP3) showed multiple bands in addition to 135-kDa expected band in the vitreous of people without diabetes and those with diabetes with various grades of DR ($n = 74$ individuals, $n = 105$ eyes; NDM controls, $n = 12$; no-mild NPDR, $n = 25$; moderate NPDR, $n = 11$; PDR, $n = 26$). The ratio of non–135-kDa/total bands increased from NDM to PDR (Fig. 1, F and G).

hRBP3 concentrations in the serum

RBP3 is highly expressed in the retina and, to a much lesser extent, in the pineal region of the brain (16, 17). Using a highly specific and sensitive ELISA (0.1 to 2 ng/ml, 1 to 15 pM), mean serum RBP3 concentration was observed at 1000- to 5000-fold lower than vitreous RBP3 concentration in NDM individuals (Fig. 2A, inset).

Intravitreous application of RBP3 in Lewis rats: Intervention study

The effect of rhRBP3 on retinal vascular function in Lewis rats was evaluated by measuring VEGF- and diabetes-induced RVP using Evan's blue dye. Doses were determined from the concentrations measured in human vitreous. Because vitreous RBP3 concentrations measured by ELISA were 1 to 2 μg/ml (8 to 16 nM) in NDM rats, 2.5 μg/ml (20 nM) of

RBP3 concentration was used for intravitreal (IVT) injection. IVT injection of rhRBP3 inhibited 200 ng/ml (7.4 nM) VEGF-induced RVP when IVT injections were given together ($P < 0.01$, premix; fig. S1C) or 1 day after VEGF injection ($P < 0.001$, intervention; fig. S1D). IVT injection of rhRBP3 in various doses (0.1 to 2.5 μg/ml, 1 to 20 nM) 1 day after VEGF (200 ng/ml) reduced VEGF-induced RVP in a dose-dependent manner with significant reduction observed at 10 and 20 nM of RBP3 ($P < 0.01$; Fig. 2B). After 2 months of diabetes, IVT injection of rhRBP3 (2.5 μg/ml, 20 nM) for 3 days reduced RVP in DM rats to those in NDM ($P < 0.01$; Fig. 2C), but boiled rhRBP3 (2.5 μg/ml, 20 nM) was not effective. Three days after IVT injection of rhRBP3, retinal mRNA expression of *Vegfa* and *Il-6* and retinal VEGFA protein expression in DM rats were significantly reduced ($P < 0.05$; Fig. 2, D and E, and fig. S1E). After 2 months of diabetes, ERG amplitudes of oscillatory potential (OP) 2, OP3, and B waves were significantly decreased compared to NDM rats ($P < 0.01$; Fig. 2F and fig. S1F). IVT injection of rhRBP3 increased amplitudes of each of these waveforms in both NDM and DM rats (Fig. 2, G to J, and fig. S1G). The presence of vitreous RBP3 at various molecular weights after IVT injection was evaluated using polyclonal antibody that recognizes both human and rodent RBP3. Immunoblot analysis of rat vitreous showed major protein bands at 25, 40, 60, 80, and 135 kDa at 10 min with and without rhRBP3 injection. After 1 day, a major band was present at 40 kDa (fig. S1, H and I). However, IVT injection of rhRBP3 for 3 days did not reverse the thinning of retinal photoreceptor layers [inner segment ellipsoid (ISE) + end tip (ET)] induced by diabetes as measured by optical coherence tomography (OCT; fig. S2, A to D).

Effects of overexpressing RBP3 on neuroretinal dysfunction induced by diabetes

The therapeutic potential for RBP3 to prevent diabetes-induced retinal dysfunction was studied by overexpressing RBP3 through subretinal injection of lentiviral vector containing either full-length hRBP3 or luciferase plasmid in Lewis rats (fig. S3, A and B). The expression of hRBP3 was increased by 85% ($P = 0.02$; Fig. 3A) and maintained for 6 months compared to control eyes (fig. S3, C to E). Diabetes decreased the endogenous expression of RBP3 protein by 53% ($P = 0.04$); however, lentiviral hRBP3 infection elevated RBP3 in the retina by 2.8-fold ($P = 0.03$) and comparable to NDM rats (Fig. 3A). Functional changes, assessed by ERG 2 months after the induction of diabetes, showed decreased amplitudes of B wave in response to light stimuli (36%; $P < 0.05$), which were prevented by overexpression of hRBP3 ($P < 0.05$; Fig. 3B). OCT assessment demonstrated that total and individual retinal layer [outer nuclear layer (ONL) and ISE + ET] thickness was decreased in DM rats compared to controls ($P < 0.05$), which were prevented especially in the photoreceptor layers by hRBP3 overexpression (ONL and ISE + ET, $P < 0.05$; Fig. 3C).

VEGF protein expression in the retina and vitreous was increased by 1.9- and 2.9-fold, respectively, in DM versus NDM rats (Fig. 3, D and E), which were completely prevented by hRBP3 overexpression (Fig. 3, D and E). Vascular permeability was increased by 2.9-fold ($P < 0.0001$) in DM rats compared to NDM controls (Fig. 3F), which was also prevented by the overexpression of hRBP3. Acellular capillary number, a classic diabetes-associated retinal pathology, was increased by 1.4-fold ($P < 0.05$) after 6 months of diabetes compared to age-matched NDM controls. Again, the overexpression of hRBP3 reduced diabetes-induced acellular capillaries by 91% ($P = 0.03$; Fig. 3G). Immunoblot analysis of retinal RBP3

protein bands exhibited at least two major bands at 80 and 135 kDa, with the fraction at 80 kDa, normalized by the total detected RBP3, increased from 26 to 52% in DM compared to NDM rats ($P < 0.001$; fig. S3, F and G).

Effects of photoreceptor-specific overexpression of RBP3

To test the therapeutic effects of RBP3 on diabetes-induced retinal dysfunction without IVT injections, we generated RBP3 transgenic (Tg) mice on a C57BL6 background that specifically over-expressed hRBP3 in photoreceptors using a rhodopsin promoter (fig. S4, A and B). Retinal mRNA and protein expressions of RBP3 were increased by 1.7-fold in RBP3 Tg mice compared to wild-type (WT) mice (Fig. 4, A and B, and fig. S4, C and D). After 2 months of streptozotocin-induced diabetes (fig. S4E), protein expressions of RBP3 in the retina were decreased by 49% ($P = 0.03$), as compared to NDM + WT mice. RBP3 mRNA and protein expressions were elevated by 1.8- and 2.1-fold ($P = 0.026$ and $P = 0.032$), respectively, in DM + RBP3Tg mice (Fig. 4, A and B), compared to DM + WT mice. Body weight and blood glucose concentrations did not differ between NDM + WT and NDM + RBP3Tg mice or between DM + WT and DM + RBP3Tg mice, although blood glucose concentrations were elevated in both DM models (fig. S4, F and G). ERG analysis of retinal function and structure using OCT demonstrated that diabetes-induced decreases in ERG amplitudes of A, B, and OP3 waves and thinning of the photoreceptor layers (ISE + ET) were not observed in DM + RBP3Tg mice (Fig. 4, C and D). The elevation in DM + WT mice of retinal *Vegf* mRNA and VEGF protein expression (Fig. 4E and fig. S4H), *Il-6* mRNA expressions (Fig. 4F), and RVP (Fig. 4G) was prevented in DM + RBP3Tg mice. Similarly, diabetes-induced formation of acellular capillaries in the retina in DM + WT mice were decreased in DM + RBP3Tg mice by 58% ($P = 0.0002$; Fig. 4H).

Effects of hRBP3 on endothelial cell migration

In bovine retinal endothelial cells (BRECs), elevating glucose concentrations from 5.6 mM [low glucose (LG)] to 25 mM [high glucose (HG)] or the addition of VEGF (2.5 ng/ml) increased cellular migration by 59% ($P < 0.05$) and 49% ($P < 0.05$), compared to LG or vehicle, respectively. The addition of rhRBP3 (0.25 μg/ml, 2 nM) inhibited HG- and VEGF-induced migration of BRECs by 50% ($P < 0.05$) and 32% ($P < 0.05$), compared to HG and VEGF, respectively (Fig. 5, A and B, and fig. S10, A and B), which were reversed by neutralizing antibodies against rhRBP3 ($P < 0.01$ and $P < 0.05$), respectively. Vitreous from a Medalist patient with NPDR, incubated with 3.1 μg/ml (23 nM) and 101.1 pg/ml of RBP3 and VEGF, respectively, completely inhibited BREC migration induced by VEGF ($P < 0.001$), and the inhibition was abolished by anti-RBP3 antibodies ($P < 0.01$; Fig. 5C and fig. S10C). Vitreous IL-6 concentration was elevated in patients with PDR (96.1 pg/ml) compared to those with NPDR (41.4 pg/ml), and its concentration in the Medalist vitreous used in the migration assay was 25.8 pg/ml.

In BRECs, RBP3 (20 nM) decreased cellular migration by 29% ($P = 0.07$), which was not significant. The addition of VEGF (2.5 ng/ml) increased cellular migration by 57% ($P = 0.01$), which was inhibited by rhRBP3 (20 nM; 48%; $P < 0.001$), whereas the addition of rhRBP3 (5 nM) did not have any effect (Fig. 5D and fig. S5A). RBP3 did not inhibit the actions of fibroblast growth factor (FGF) to induce EC migrations (fig. S5B).

Structurally, RBP3 has four distinct domains: The first domain (D1; amino acids 19 to 320, 34 kDa) has some similarities to other retinol binding proteins (RBP1, RBP2, RBP4, and RBP5), and the second domain (D2; amino acids 321 to 630, 35 kDa) is known to have lipid binding sites. The effects of D1 and D2 (20 nM) on VEGF-induced migration were studied (13, 18, 19). ECs were incubated with vehicle, rhRBP4, rhRBP3 (full; amino acids 1 to 1247, 135 kDa), rhRBP3 (D1), rhRBP3 (D2), or rhRBP3 (D1 + D2). VEGF increased EC migration ($P < 0.05$). However, RBP3 (20 nM) inhibited VEGF-induced migration by 47% ($P < 0.0001$). D1, D2, and combination of D1 and D2 inhibited VEGF-induced EC migration by 51, 37, and 45%, ($P < 0.0001$, $P < 0.0001$, and $P < 0.0001$), respectively (all 20 nM; Fig. 5E and fig. S5C). D1 consistently inhibited VEGF-induced migration more than D2 ($P < 0.05$), and the inhibitory effect of D1 was similar to the full length of hRBP3 and D1 + D2 (Fig. 5E and fig. S5C). RBP4 (20 nM) did not inhibit VEGF-induced migration.

Effects of rhRBP3 on VEGFR2 signaling

Preincubation of rhRBP3 (0.25 μg/ml, 2 nM) with VEGF (2.5 ng/ml) inhibited VEGF-induced pTyr-VEGFR2 in BRECs ($P < 0.01$), whereas co-addition of rhRBP3 did not (Fig. 5F). To test the hypothesis that RBP3 inhibited VEGF-induced pTyr-VEGFR2, by binding to VEGFR2, we coincubated cells with rhRBP4, rhRBP3, or phosphate-buffered saline (PBS) with reversible cross-linkers (DTSSP), and cell lysate was immunoprecipitated (IP) with anti-VEGFR2 antibody and then blotted with anti–tyrosine phosphorylation antibody. Immunoblot analysis showed that rhRBP3 (20 nM) inhibited VEGF (2.5 ng/ml)–induced pTyr-VEGFR2 by 25% ($P < 0.01$) but had no effect when cells were treated with VEGF (25 ng/ml). rhRBP4 (20 nM) was ineffective (Fig. 5G).

Effects of rhRBP3 on HG-induced VEGF expression

rhRBP3 (20 nM) reduced mRNA expression of *Vegf* and *Il-6*, as well as HG-induced protein expression of VEGF in Müller cells, the primary retinal cell type responsible for their production in diabetes (20). Although rhRBP3 at 0.5 μg/ml reduced *Vegf* mRNA expression induced by HG, it did not alter VEGFA protein expression (Fig. 6, A and B, and fig. S6, A to C). RhRBP3 also reduced HG-induced mRNA expression of *Vegfa* and *Il-6* in BRECs (fig. S6, D and E).

To determine the mechanism by which RBP3 inhibits HG-induced *Vegf* and *Il-6* mRNA expression, we studied the role of glucose transporter expression in Müller cells. Potential glucose transporters were screened by measuring the expression of multiple transporter genes (*Glut1*, *Glut4*, *Sglt1*, and *Sglt2*) by quantitative reverse transcription polymerase chain reaction. We found that *Glut1* is dominantly expressed in Müller cells (fig. S7A). In addition, HG-induced migration was inhibited by a glucose transporter 1 (GLUT1) selective inhibitor (STF31) in ECs (fig. S7B). The role of GLUT1 in mediating HG-induced increases in VEGF and IL-6 mRNA and protein expression was supported by STF31 inhibition of HG-induced expression of these cytokines (Fig. 6, A and B, and fig. S6, A to C). Further, in cross-linking experiments, Müller cells were coincubated with BSA, boiled rhRBP3, or rhRBP3 with either reversible DTSSP or the irreversible cross-linker formaldehyde. Then, cellular membranes were isolated and IP with anti-GLUT1 or anti-RBP3 antibody.

Immunoblot analysis showed selective association with GLUT1 but not with BSA or boiled rhRBP3 (Fig. 6, C to E).

Effects of rhRBP3 on 3-*O*-methyl-D-glucose and 2-deoxy-D-glucose uptake

Because rhRBP3 may bind to GLUT1 transporters, the effect of rhRBP3 on 3-*O*-methyl-D-glucose (3-*O*-MG) and 2-deoxy-D-glucose (2DG) uptake was studied after incubating Müller cells and BRECs with rhRBP3 for 1 hour. RhRBP3 inhibited [^{3}H]3-*O*-MG uptake by 65.4 and 65.0% compared with PBS in Müller cell and BRECs ($P < 0.01$ and $P < 0.001$), respectively (Fig. 7A and fig. S7C). RhRBP3 (5 μg/ml) also inhibited [^{3}H]2DG uptake by 74, 26, and 62% compared with PBS in Müller cells, BRECs, and Y79 cells ($P < 0.001$, $P < 0.0001$, and $P < 0.001$), respectively; [^{3}H]2DG uptake was also reduced by 71, 45, and 83% by STF31 ($P < 0.001$, $P < 0.0001$, and $P < 0.0001$) compared with PBS, respectively, but not by BSA or boiled rhRBP3 (5 μg/ml; Fig. 7, B to D). RhRBP3 also inhibited [^{3}H]2DG uptake in a dose-dependent manner from 0.05 to 5.0 μg/ml range, and its inhibitory actions by rhRBP3 (5 μg/ml) were reduced by the addition of anti-RBP3 antibodies in Müller cells, BRECs, and Y79 cells ($P < 0.001$, $P < 0.0001$, and $P < 0.05$), respectively (Fig. 7, B to D). In contrast, rhRBP3 did not inhibit [^{3}H]2DG uptake into human retinal pigment epithelial cells (RPEs; Fig. 7E). rhRBP3 (5 ng/ml) did not inhibit [^{3}H]2DG uptake into undifferentiated and differentiated C2C12 and adipocytes (fig. S7, D to G). The concentration of rhRBP3 (5 ng/ml) used for this experiment was comparable to physiological serum concentrations of RBP3 (0.4 to 4 ng/ml or 3 to 30 pM) based on the results from ELISA (Fig. 2A). Vitreous from Medalist patients with PDR (low RBP3, 5.0 ± 0.6 nM) inhibited [^{3}H]2DG glucose uptake in Müller cells much less than vitreous from NPDR individuals (high RBP3, 15.7 ± 2.2 nM) ($P < 0.01$; fig. S8A).

Effects of rhRBP3 of different structural domains on 2DG uptake

The effects of D1 and D2 (40 nM) on 2DG uptake were studied after the incubation of Müller cells with D1 and D2 for 1 hour. Full-length rhRBP3 (5 μg/ml, 40 nM) inhibited [^{3}H]2DG uptake by 44% ($P < 0.0001$), whereas D1, D2, and the combination of D1 and D2 inhibited 34, 19, and 36%, ($P < 0.0001$, $P < 0.0001$, and $P < 0.0001$), compared with PBS, respectively. D1 inhibited [^{3}H]2DG uptake significantly more than D2 ($P < 0.05$), whereas D1 + D2 combination had inhibitory effects similar to D1, and rhRBP4 (40 nM) had no effect (Fig. 7F). Cross-linking experiments with DTSSP showed that full-length rhRBP3 or D1 inhibited VEGF-induced pTyr-VEGFR2, whereas rhRBP4 and D2 had no effect (fig. S8B).

Effects of hRBP3 on extracellular acidification rate in Müller cells and mouse retina

Because rhRBP3 could be decreasing glucose uptake in retinal Müller cells and ECs, we determined its effects on glycolytic rates by measuring extracellular acidification using the seahorse apparatus (21). ECAR analysis of vehicle-treated Müller cells showed that LG (5.6 mM) increases basal ECAR by 1.7-fold ($P < 0.05$), which was increased further by HG (25 mM) to 2.0-fold ($P < 0.001$), compared to basal ECAR. For control, ECAR was maximized by 5.2-fold with addition of a combination of RAA, inhibitor of mitochondria complexes I and III ($P < 0.0001$), compared to basal ECAR, and reduced by 2DG ($P < 0.001$), compared to ECAR by RAA (Fig. 7G). The basal ECAR and maximal ECAR by RAA were inhibited

by rhRBP3 (5.0 μg/ml; $P < 0.01$ and $P < 0.01$) compared to boiled rhRBP3 (5.0 μg/ml), respectively (Fig. 7G). In contrast, rhRBP3 did not affect palmitate's effect on oxygen consumption ratio (OCR) in Müller cells (fig. S8C).

Analysis of ECAR in the isolated retina of NDM + WT or DM + WT and RBP3Tg mice was performed. ECAR analysis of NDM + WT showed that LG, HG, and RAA increased ECAR by 2.2-, 2.1-, and 2.3-fold ($P < 0.001$, $P < 0.0001$, and $P < 0.0001$), compared to basal ECAR, respectively, and reduced by 2DG ($P < 0.01$), compared to ECAR by RAA. Basal ECAR and LG- and HG-induced ECAR in DM + WT mice were increased by 1.7-, 1.6-, and 1.5-fold ($P < 0.001$, $P < 0.01$, and $P < 0.001$), respectively, compared to ECAR in NDM + WT mice. ECAR in DM + WT mice was consistently increased by 1.6- and 1.6-fold with RAA and 2DG ($P < 0.001$ and $P < 0.01$), respectively, compared to ECAR in NDM + WT mice. There was no difference in ECAR between NDM + WT mice and NDM + RBP3Tg mice. However, basal ECAR and LG- and HG-induced ECAR in the retina of DM + RBP3Tg mice were reduced by 33, 30, and 32% ($P < 0.01$, $P < 0.01$, and $P < 0.01$), respectively, compared to those of DM + WT mice. Consistently, ECAR in DM + RBP3Tg mice was reduced by 36 and 31% with RAA and 2DG ($P < 0.001$ and $P < 0.05$), respectively, compared to those of DM + WT mice (Fig. 7H).

DISCUSSION

This study suggests that RBP3 may play a major role in protecting against the development of severe DR through its ability to ameliorate the actions of hyperglycemia on retinal ECs and Müller cells. Critical to this study was the availability of retina and vitreous from Medalist patients, which allowed for screening for potential protective factors that neutralize the adverse effects of hyperglycemia on the progression of DR. From the candidate proteins up-regulated in the retina and vitreous of Medalist patients with no-mild NPDR, RBP3 was selected for further study due to its specific expression to the photoreceptors and its unique function. RBP3 was also selected because its expression has been reported to decrease in DR (14). RBP3 is a large 135-kDa secreted protein produced mainly in the photoreceptors with a well-established function of binding and transporting cis/trans retinols between photoreceptors and RPE (16, 22). Further, RBP3 protein structures have separate domains of binding for retinols and lipids. RBP3 may have retinol trophic actions because people with RBP3 mutations develop retinal degeneration (12).

Our findings showed that there was an about five fold decrease in RBP3 expression in the retina and vitreous in people with severe DR compared to NDM eyes. This marked reduction of RBP3 in the vitreous was related to the severity of DR and likely related to the extent of hyperglycemia. This conclusion is based on the finding that RBP3 expression was decreased in the retina of DM mice. RBP3 concentrations in the vitreous of people with type 1 or type 2 diabetes exhibit gradual decreases from the highest expression in no DR to the lowest expression in severe NPDR. In addition, a previous study reported a relative reduction of RBP3 expressions in the vitreous of people with type 2 diabetes by immunoblot analysis (14), and the authors suggested that this decrease in RBP3 could be due to hyperglycemia and, possibly, elevated inflammatory cytokines. It is unlikely that the reduction of RBP3 in the vitreous is due to loss of the photoreceptor layer resulting from laser panretinal

photocoagulation, because RBP3 reduction occurred with severe NPDR before photocoagulation procedures. With the development of a highly selective and sensitive ELISA, we were able to measure serum RBP3 concentration and directly compare to vitreous RBP3 expression in the same individual, which showed that RBP3 in serum is 1000 times less concentrated than in vitreous. This is expected, given that RBP3 is predominately produced in the retina and the observed dilution factor is consistent with the ratio of vitreous volume to serum volume (16, 17).

Analysis of the relationship between RBP3, VEGF, and IL-6 in the vitreous indicated that RBP3 concentrations were inversely correlated with the inflammatory cytokines with their ratios decreasing with increasing severity of DR. These findings suggest that ratios of RBP3 and VEGF or IL-6 in the vitreous might be a potential indicator of resistance to development of advanced DR (23). However, circulating VEGF and IL-6 concentrations are not reflective of retinal changes because both are secreted by many tissues. Future studies are needed to evaluate the utility of serum RBP3 as a biomarker for the progression of DR.

Immunoblot analysis of RBP3 expression in the vitreous and retina of rodents and people yielded multiple bands of proteins at 100, 80, and 40 kDa. These findings suggest that there is substantial degradation of RBP3 under physiological conditions, which is exacerbated by the presence of diabetes. This idea is supported by the findings of elevated concentrations of the smaller molecular weight bands in the vitreous of people with PDR and in the retina of rodents with increased DM duration. The finding of discrete bands of similar molecular weight in people and rodents also suggests that specific proteases in the retina could be involved and their expressions can be enhanced by diabetes. These findings also indicate that degradation of RBP3 may be an additional mechanism for regulation of its physiological actions in the retina.

This study has identified several actions of RBP3, a secreted neuroretinal protein that may have direct effects on other retinal cells and vasculature. There is great interest in the role of neuroretinal abnormalities on the development of DR because neuroretinal changes detected by ERG have been reported to precede vascular pathologies in DR (24, 25). Until now, no direct molecular signaling mechanism has been identified between the neuroretina and the vascular retina that affected progression of DR (26). Evaluation of RBP3 by the intravitreous administration or its overexpression in DM Tg rodent models showed that elevating RBP3 to physiological concentrations (20 nM) can prevent and even reverse vascular permeability and other retinal abnormalities, such as the decreases in neuroretinal responses measured by ERG, induced by diabetes. IVT injection of RBP3 appears to increase ERG amplitude, but the overexpression of RBP3 in the retina did not change ERG. This could be related to the duration of the increases in RBP3 exposure, which was assessed in 3 days after IVT injection, whereas the overexpression models were studied after 2 to 3 months.

There may be multiple mechanisms by which RBP3 exerts protective actions. One mechanism suggests that RBP3 can inhibit pTyr- VEGFR2, possibly by blocking VEGF binding to VEGFR2. However, the unexpected finding that RBP3 can reduce the expression of VEGF and IL-6 may indicate that RBP3 actions are broader than simply blocking VEGF actions. RBP3 may decrease glucose uptake and metabolism in several, but not all, retinal

cell types, possibly by binding to GLUT1. Results from the retinal cell–based assays demonstrated that hyperglycemia increased the expression of VEGF and IL-6 via GLUT1, the major glucose transporter in Müller cells, because the effects of HG were inhibited by the GLUT1-selective inhibitor, STF31. Under physiological concentrations, RBP3 inhibited glucose transport and uptake in the retinal cells. However, at lower concentrations comparable to those detected with increasing severe DR, inhibitory actions of RBP3 on glucose uptake were decreased. GLUT1-specific inhibitor, STF31, inhibited the effect of HG on ECs and Müller cells equally as RBP3, strongly suggesting that the inhibitory actions of RBP3 are mainly mediated by decreasing glucose uptake via GLUT1. Further, RBP3 selectively cross-linked with GLUT1 and inhibited glycolysis in the presence of HG in Seahorse assays in Müller cells and intact retina from WT and RBP3Tg mice. However, the inhibitory effects of RBP3 on glucose transport are selective, because RBP3 was not effective at reducing glucose uptake in RPE, adipocytes, and skeletal cells. In addition, RBP3 did not alter the effects of palmitate, a fatty acid, as measured by OCR.

The mechanisms underlying the selectivity of RBP3 binding and inhibition of glucose uptake in various cells are related to its binding to GLUT1. Systemic action on glucose metabolism by RBP3 is unlikely because serum RBP3 concentrations are more than thousand times lower than its inhibitory concentration. In the retina, inhibitory actions of RBP3 on glucose uptake are partial and may be more active during HG than in LG conditions. It is unlikely that RBP3 inhibitory actions on GLUT1 at normal concentrations of glucose will have substantial effect on retinal fuel consumptions because individuals with GLUT1 gene defects have no reported any visual defects, although they exhibit neurological pathologies and seizures (27).

Another protective action of RBP3 appears to be its binding to VEGFR2 as shown by its reduction of pTyr-VEGFR2. RBP3's binding to VEGFR2 is likely dependent on the ambient retinal concentration of VEGF and RBP3, as suggested by the correlation of RBP3/ VEGF ratio in the vitreous to the severity of DR. This is supported by the finding that IVT injection of VEGF at 200 ng/ml induced RVP even in the presence of 1 to 2 μg/ml (8 to 16 nM) of endogeneous RBP3. This is further supported by the dose-response studies, showing that median inhibitory concentration of RBP3 is between 0.7 to 2.0 μg/ml (5 to 16 nM) with its concentrations in PDR at 0.5 to 1.0 μg/ml (4 to 8 nM), which is at the low end of its actions. In dose-response studies, RBP3 concentrations at 1 to 2.5 μg/ml were required to inhibit vascular permeability induced by VEGF in the retina. In addition, vitreous from Medalist patients with NPDR (high RBP3, 15.7 ± 2.2 nM) and PDR (low RBP3, 5.0 ± 0.6 nM) showed that the vitreous from PDR individuals was not as effective as vitreous from NPDR individuals.

The mechanism of RBP3 binding to GLUT1 and possibly other cell surface proteins such as VEGFR2 is selective but not specific because our data have shown that RBP3 could bind to both GLUT1 and VEGFR2 but not FGF or fatty acid transporters. RBP3 has at least two retinol binding domains and a separate and evolutionarily conserved domain that may bind other lipids (13, 18). There has been speculation that RBP3 may have other retinal functions besides transporting cis/trans retinols, because mutations in RBP3 genes cause retinal degeneration, which has also been observed in mice with deletion of the RBP3 gene (11).

Cross-linkage and structure/functional analysis showed that RBP3 can bind to VEGFR2 receptors but cannot inhibit the actions of FGF. Further, 34-kDa fragment of RBP3 (amino acids 19 to 320; D1) inhibited 2DG glucose uptake and VEGF-induced migration better than another RBP3 fragment containing D2 (amino acids 321 to 630). Experiments using reversible cross-linker also showed that full-length RBP3, as well as D1, inhibited VEGF-induced pTyr-VEGFR2 better than D2. These findings indicated that protective actions of RBP3 may be mediated selectively via binding to GLUT1 and VEGFR2, possibly via the retinol binding regions of RBP3. These new findings on the structure/function properties of the RBP3 and two different domains of RBP3 (D1 and D2) strengthen the mechanistic relationship between RBP3, GLUT1, and VEGFR2. Future studies will be needed to determine whether RBP3 can bind to other cell surface proteins using similar or other domains.

There are several limitations to this study. The patients with diabetes studied here were mostly people with long duration of type 1 diabetes. The results will need to be replicated in people with type 1 diabetes of short duration and those with type 2 diabetes. In addition, more precise definition for the mechanism of RBP3 on its effects to decrease the toxic actions of hyperglycemia is needed.

In summary, we have found that preservation of RBP3, through either supplementation or increased expression from the photoreceptors, can protect neuroretina and vascular retina from diabetes-induced retinal dysfunction and pathology. This protective activity is partially mediated by RBP3 binding to GLUT1 and inhibition of glucose uptake in retinal cells, with subsequent decreased expression of VEGF and inflammatory cytokines. These results provide evidence of a definitive pathway from the neuroretina that can regulate vascular retinal glucose metabolism and function in the DM eye.

MATERIALS AND METHODS

Study design

The Joslin 50-year Medalist Study consists of participants recruited from across 50 states in the United States between 2004 and 2019. Participants were included in the study if they had ≥50 years of well-documented type 1 diabetes at time of recruitment. The Medalist Study has been previously described in detail (9, 10). All Medalist patients were extensively characterized at Joslin Diabetes Center (JDC) through detailed history, clinical and ophthalmologic examinations, and biospecimen collections. Several Medalist patients also consented to postmortem organ donations. The goal of this study is to identify factors in the retina or vitreous that are associated with resistance to the initiation or progression of retinopathy in the presence of hyperglycemia. By 2010, we had gathered 17 eyes through these postmortem eye donations. For our initial pilot and feasibility study at this time, proteomic analysis was performed in donated retinas and vitreous postmortem samples from Medalist patients diagnosed with only no-mild NPDR (n = 6 eyes and n = 4 individuals) and compared to those with PDR (n = 11 eyes and n = 6 individuals). Both groups had comparable HbA1c. These numbers were based on a previous comparable vitreous proteomic study performed by the Joslin mass spectroscopy core (28). Validation (via ELISA and immunoblot analysis) and replication studies of RBP3, the candidate protein that

emerged from this initial pilot study, were then conducted on the basis of using a larger pool of all the available postmortem and alive vitreous samples collected from Medalist patients by 2017. Through collaborative efforts of the Beetham Eye Clinic at JDC, as well as California Retina Consultants and other tissue procurement networks, we also procured postmortem and alive vitreous samples from non-Medalist patients, including type 1 diabetes, type 2 diabetes, and NDM controls, all of whom had known DR status (NDM, no-mild NPDR, moderate NPDR, and PDR). These samples were also included in our validation and replication studies of RBP3. The grading of DR in the replication sets was performed in a shielded manner. Although all available samples were used for the ELISA, the immunoblot studies were performed in a subset of the replication cohort due to the limitations of biospecimen quantity available. Along with RBP3, vitreous VEGF concentrations were also assessed by ELISA in the replication sets. For the various animal models used in this investigation, we reported the number of replication experiments or number of mice and rats in the figure legends.

As described previously (9, 10) at initial visit, Medalist patients were evaluated at the JDC by medical history questionnaire and clinical and ophthalmic examination, and biospecimens were collected. HbA1c was determined by high-performance liquid chromatography (Tosoh, Tokyo, Japan), and lipid profiles by enzymatic methods (Roche Diagnostics, Indianapolis, IN and Denka Seiken and Asahi Kasei, Tokyo, Japan). Dilated eye examination was performed, and DR was graded on Early Treatment Diabetic Retinopathy Study protocol 7 standard field stereoscopic fundus photographs (29). Institutional review boards at the JDC and each participating site approved the study protocols.

Statistical analysis

Comparisons among two groups were made with independent sample t tests. For comparisons of more than two groups, ANOVA was used. When overall F tests were significant, pairwise comparisons were examined using Fisher's least significant difference test. When data exhibited significant lack of normality, nonparametric analogs (such as Mann-Whitney U test) were used. Association between continuous variables was assessed with linear regression. When repeated measures were made within individuals (such as rat subretinal injection experiments; fig. S3C), linear mixed-effects models were performed. Statistical significance was determined a priori because $P < 0.05$ and all statistical tests were two-sided. Analysis was performed using SAS v9.4, and figures were produced using GraphPad Prism software. Fold change in peptide expression was calculated by the ratio in the more severe disease group to the no-mild DR group in human studies and of the experimental groups to control in in vivo studies. The eyes were treated as independent observations. In rat experiments, animals with dense cataracts or whole corneal defects were excluded from analysis due to inability to obtain reliable optical results. Significance was defined as $*P < 0.05$, $**P < 0.01$, $***P < 0.001$, and $****P < 0.0001$.

Supplementary Material

Refer to Web version on PubMed Central for supplementary material.

Acknowledgments

We thank the Medalists patients and their families, the individuals who donated eye samples, the clinicians at the Beetham Eye Institute, the National Disease Research Interchange (NDRI), and the California Retina Consultants (R.L.A.) for coordinating eye donations, the Medalist staff (S. Turek, S. D'Eon, and S. Hastings), the Proteomics Core staff (X. Chen and J. Woodward), and B. Kunkemoeller, Y.-H. Tseng, and S. Kissler at the JDC.

Funding: This work was supported by grants from the NIH NEI R01EY026080-01 to G.L.K., National Institute of Diabetes and Digestive and Kidney Diseases (NIDDK) NIH 1DP3DK112192-01 to G.L.K. and NIH 1DP3DK094333-01 to G.L.K. and H.A.K., and NIDDK Diabetes Research Center grant P30DK036836; grants from the Juvenile Diabetes Research Foundation (JDRF) JDRF 8-2005-358 (G.L.K.), JDRF 18-2008-363 (G.L.K.), JDRF17-2011-474 (H.A.K.), and JDRF17-2013-310 (H.A.K.); and a grant from the Beatson Foundation Gift and the Dianne Nunnally Hoppes fund. H.Y. received the research fellowship from Manpei Suzuki Diabetes Foundation, Japan, and Mary K. Iacocca Foundation, USA. G.L.K. had held a basic research grant from Sanofi pharmaceutical company during part of this study. The support from Sanofi was for renal studies and not applicable to the studies on RBP3 or eyes in the Medalist study.

REFERENCES AND NOTES

1. Leasher JL, Bourne RRA, Flaxman SR, Jonas JB, Keeffe J, Naidoo K, Pesudovs K, Price H, White RA, Wong TY, Resnikoff S, Taylor HR, Global estimates on the number of people blind or visually impaired by diabetic retinopathy: A meta-analysis from 1990 to 2010. Diabetes Care 39, 1643–1649 (2016). [PubMed: 27555623]
2. Das A, Diabetic retinopathy: Battling the global epidemic. Invest. Ophthalmol. Vis. Sci 57, 6669–6682 (2016). [PubMed: 27936469]
3. Yau JWY, Rogers SL, Kawasaki R, Lamoureux EL, Kowalski JW, Bek T, Chen S-J, Dekker JM, Fletcher A, Grauslund J, Haffner S, Hamman RF, Ikram MK, Kayama T, Klein BEK, Klein R, Krishnaiah S, Mayurasakorn K, O'Hare JP, Orchard TJ, Porta M, Rema M, Roy MS, Sharma T, Shaw J, Taylor H, Tielsch JM, Varma R, Wang JJ, Wang N, West S, Xu L, Yasuda M, Zhang X, Mitchell P, Wong TY; Meta-Analysis for Eye Disease (META-EYE) Study Group, Global prevalence and major risk factors of diabetic retinopathy. Diabetes Care 35, 556–564 (2012). [PubMed: 22301125]
4. Olsen TW, Anti-VEGF pharmacotherapy as an alternative to panretinal laser photocoagulation for proliferative diabetic retinopathy. JAMA 314, 2135–2136 (2015). [PubMed: 26565713]
5. Martin DF, Maguire MG, Treatment choice for diabetic macular edema. N. Engl. J. Med 372, 1260–1261 (2015). [PubMed: 25692914]
6. Amoaku WMK, Saker S, Stewart EA, A review of therapies for diabetic macular oedema and rationale for combination therapy. Eye 29, 1115–1130 (2015). [PubMed: 26113500]
7. Rask-Madsen C, King GL, Vascular complications of diabetes: Mechanisms of injury and protective factors. Cell Metab. 17, 20–33 (2013). [PubMed: 23312281]
8. Qi W, Keenan HA, Li Q, Ishikado A, Kannt A, Sadowski T, Yorek MA, Wu I-H, Lockhart S, Coppey LJ, Pfenninger A, Liew CW, Qiang G, Burkart AM, Hastings S, Pober D, Cahill C, Niewczas MA, Israelsen WJ, Tinsley L, Stillman IE, Amenta PS, Feener EP, Vander Heiden MG, Stanton RC, King GL, Pyruvate kinase M2 activation may protect against the progression of diabetic glomerular pathology and mitochondrial dysfunction. Nat. Med 23, 753–762 (2017). [PubMed: 28436957]
9. Keenan HA, Costacou T, Sun JK, Doria A, Cavellerano J, Coney J, Orchard TJ, Aiello LP, King GL, Clinical factors associated with resistance to microvascular complications in diabetic patients of extreme disease duration: The 50-year Medalist study. Diabetes Care 30, 1995–1997 (2007). [PubMed: 17507696]
10. Sun JK, Keenan HA, Cavallerano JD, Asztalos BF, Schaefer EJ, Sell DR, Strauch CM, Monnier VM, Doria A, Aiello LP, King GL, Protection from retinopathy and other complications in patients with type 1 diabetes of extreme duration: The Joslin 50-year Medalist study. Diabetes Care 34, 968–974 (2011). [PubMed: 21447665]
11. Liou GI, Fei Y, Peachey NS, Matragoon S, Wei S, Blaner WS, Wang Y, Liu C, Gottesman ME, Ripps H, Early onset photoreceptor abnormalities induced by targeted disruption of the

interphotoreceptor retinoid-binding protein gene. J. Neurosci 18, 4511–4520 (1998). [PubMed: 9614228]

12. den Hollander AI, McGee TL, Ziviello C, Banfi S, Dryja TP, Gonzalez-Fernandez F, Ghosh D, Berson EL, A homozygous missense mutation in the IRBP gene (RBP3) associated with autosomal recessive retinitis pigmentosa. Invest. Ophthalmol. Vis. Sci 50, 1864–1872 (2009). [PubMed: 19074801]
13. Gonzalez-Fernandez F, Bevilacqua T, Lee K-I, Chandrashekar R, Hsu L, Garlipp MA, Griswold JB, Crouch RK, Ghosh D, Retinol-binding site in interphotoreceptor retinoid-binding protein (IRBP): A novel hydrophobic cavity. Invest. Ophthalmol. Vis. Sci 50, 5577–5586 (2009). [PubMed: 19608538]
14. Garcia-Ramírez M, Hernández C, Villarroel M, Canals F, Alonso MA, Fortuny R, Masmiquel L, Navarro A, García-Arumí J, Simó R, Interphotoreceptor retinoid-binding protein (IRBP) is downregulated at early stages of diabetic retinopathy. Diabetologia 52, 2633–2641 (2009). [PubMed: 19823802]
15. Tinsley LJ, Kupelian V, D'Eon SA, Pober D, Sun JK, King GL, Keenan HA, Association of glycemic control with reduced risk for large-vessel disease after more than 50 years of type 1 diabetes. J. Clin. Endocrinol. Metab 102, 3704–3711 (2017). [PubMed: 28973526]
16. Gonzalez-Fernandez F, Ghosh D, Focus on molecules: Interphotoreceptor retinoid-binding protein (IRBP). Exp. Eye Res 86, 169–170 (2008). [PubMed: 17222825]
17. Rodrigues MM, Hackett J, Gaskins R, Wiggert B, Lee L, Redmond M, Chader GJ, Interphotoreceptor retinoid-binding protein in retinal rod cells and pineal gland. Invest. Ophthalmol. Vis. Sci 27, 844–850 (1986). [PubMed: 3700035]
18. Ghosh D, Haswell KM, Sprada M, Gonzalez-Fernandez F, Structure of zebrafish IRBP reveals fatty acid binding. Exp. Eye Res 140, 149–158 (2015). [PubMed: 26344741]
19. Ghosh D, Haswell KM, Sprada M, Gonzalez-Fernandez F, Fold conservation and proteolysis in zebrafish IRBP structure: Clues to possible enzymatic function? Exp. Eye Res 147, 78–84 (2016). [PubMed: 27155144]
20. Wang J, Xu X, Elliott MH, Zhu M, Le Y-Z, Müller cell-derived VEGF is essential for diabetes-induced retinal inflammation and vascular leakage. Diabetes 59, 2297–2305 (2010). [PubMed: 20530741]
21. Mookerjee SA, Gerencser AA, Nicholls DG, Brand MD, Quantifying intracellular rates of glycolytic and oxidative ATP production and consumption using extracellular flux measurements. J. Biol. Chem 292, 7189–7207 (2017). [PubMed: 28270511]
22. Jin M, Li S, Nusinowitz S, Lloyd M, Hu J, Radu RA, Bok D, Travis GH, The role of interphotoreceptor retinoid-binding protein on the translocation of visual retinoids and function of cone photoreceptors. J. Neurosci 29, 1486–1495 (2009). [PubMed: 19193895]
23. Koskela UE, Kuusisto SM, Nissinen AE, Savolainen MJ, Liinamaa MJ, High vitreous concentration of IL-6 and IL-8, but not of adhesion molecules in relation to plasma concentrations in proliferative diabetic retinopathy. Ophthalmic Res. 49, 108–114 (2013). [PubMed: 23257933]
24. Luu CD, Szental JA, Lee S-Y, Lavanya R, Wong TY, Correlation between retinal oscillatory potentials and retinal vascular caliber in type 2 diabetes. Invest. Ophthalmol. Vis. Sci 51, 482–486 (2010). [PubMed: 19710418]
25. Pescosolido N, Barbato A, Stefanucci A, Buomprisco G, Role of electrophysiology in the early diagnosis and follow-up of diabetic retinopathy. J. Diabetes Res 2015, 319692 (2015). [PubMed: 26075282]
26. Moran EP, Wang Z, Chen J, Sapieha P, Smith LEH, Ma J.-x., Neurovascular cross talk in diabetic retinopathy: Pathophysiological roles and therapeutic implications. Am. J. Physiol. Heart Circ. Physiol 311, H738–H749 (2016). [PubMed: 27473938]
27. Sen S, Keough K, Gibson J, Clinical reasoning: Novel GLUT1-DS mutation: Refractory seizures and ataxia. Neurology 84, e111–e114 (2015). [PubMed: 25870456]
28. Gao B-B, Chen X, Timothy N, Aiello LP, Feener EP, Characterization of the vitreous proteome in diabetes without diabetic retinopathy and diabetes with proliferative diabetic retinopathy. J. Proteome Res 7, 2516–2525 (2008). [PubMed: 18433156]

29. Early Treatment Diabetic Retinopathy Study Research Group, Fundus photographic risk factors for progression of diabetic retinopathy. ETDRS report number 12. Ophthalmology 98, 823–833 (1991). [PubMed: 2062515]
30. Geraldes P, Hiraoka-Yamamoto J, Matsumoto M, Clermont A, Leitges M, Marette A, Aiello LP, Kern TS, King GL, Activation of PKC-δ and SHP-1 by hyperglycemia causes vascular cell apoptosis and diabetic retinopathy. Nat. Med 15, 1298–1306 (2009). [PubMed: 19881493]
31. Liang C-C, Park AY, Guan J-L, In vitro scratch assay: A convenient and inexpensive method for analysis of cell migration in vitro. Nat. Protoc 2, 329–333 (2007). [PubMed: 17406593]
32. Rask-Madsen C, King GL, Differential regulation of VEGF signaling by PKC-α and PKC-ε in endothelial cells. Arterioscler. Thromb. Vasc. Biol 28, 919–924 (2008). [PubMed: 18323518]
33. Park K, Li Q, Evcimen ND, Rask-Madsen C, Maeda Y, Maddaloni E, Yokomizo H, Shinjo T, St-Louis R, Fu J, Gordin D, Khamaisi M, Pober D, Keenan H, King GL, Exogenous insulin infusion can decrease atherosclerosis in diabetic rodents by improving lipids, inflammation, and endothelial function. Arterioscler. Thromb. Vasc. Biol 38, 92–101 (2018). [PubMed: 29162603]
34. Schmittgen TD, Livak KJ, Analyzing real-time PCR data by the comparative CT method. Nat. Protoc 3, 1101–1108 (2008). [PubMed: 18546601]
35. Park K, Li Q, Rask-Madsen C, Mima A, Mizutani K, Winnay J, Maeda Y, D'Aquino K, White MF, Feener EP, King GL, Serine phosphorylation sites on IRS2 activated by angiotensin II and protein kinase C to induce selective insulin resistance in endothelial cells. Mol. Cell. Biol 33, 3227–3241 (2013). [PubMed: 23775122]
36. Clermont A, Chilcote TJ, Kita T, Liu J, Riva P, Sinha S, Feener EP, Plasma kallikrein mediates retinal vascular dysfunction and induces retinal thickening in diabetic rats. Diabetes 60, 1590–1598 (2011). [PubMed: 21444925]
37. Katagiri S, Park K, Maeda Y, Rao TN, Khamaisi M, Li Q, Yokomizo H, Mima A, Lancerotto L, Wagers A, Orgill DP, King GL, Overexpressing IRS1 in endothelial cells enhances angioblast differentiation and wound healing in diabetes and insulin resistance. Diabetes 65, 2760–2771 (2016). [PubMed: 27217486]
38. Clermont A, Murugesan N, Zhou Q, Kita T, Robson PA, Rushbrooke LJ, Evans DM, Aiello LP, Feener EP, Plasma kallikrein mediates vascular endothelial growth factor-induced retinal dysfunction and thickening. Invest. Ophthalmol. Vis. Sci 57, 2390–2399 (2016). [PubMed: 27138737]
39. Kissler S, Stern P, Takahashi K, Hunter K, Peterson LB, Wicker LS, In vivo RNA interference demonstrates a role for Nramp1 in modifying susceptibility to type 1 diabetes. Nat. Genet 38, 479–483 (2006). [PubMed: 16550170]
40. Kern TS, Miller CM, Du Y, Zheng L, Mohr S, Ball SL, Kim M, Jamison JA, Bingaman DP, Topical administration of nepafenac inhibits diabetes-induced retinal microvascular disease and underlying abnormalities of retinal metabolism and physiology. Diabetes 56, 373–379 (2007). [PubMed: 17259381]

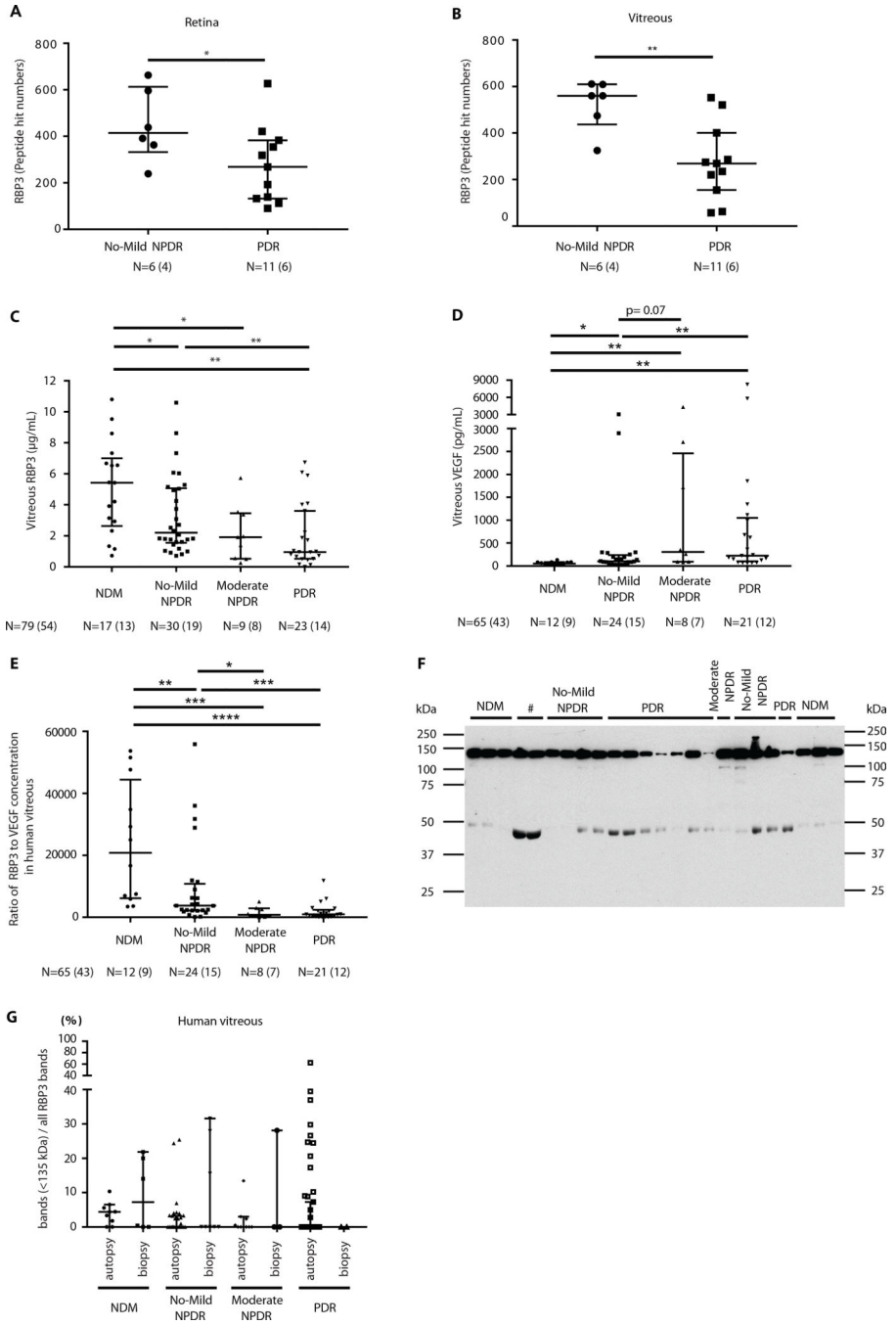

Fig. 1. Measurement of RBP3 peptide and protein expression and its correlation of VEGF in human vitreous of different grades of DR.

(**A** and **B**) Proteomic analysis of RBP3 in Medalist patients with no-mild NPDR (protected eyes) and those with PDR (nonprotected eyes) in the retina and vitreous. (**C** and **D**) Vitreous RBP3 and VEGF concentration in the mixed population of individuals with type 1 and type 2 diabetes and without diabetes (NDM). (**E**) The ratio of RBP3 to VEGF concentration in vitreous. (**F**) Representative immunoblot (IB) for RBP3 expression (#, ungradable) in human vitreous and (**G**) quantification of degraded RBP3 by ratio of RBP3 bands (<135 kDa) to all

RBP3 bands. n = numbers of eyes (individuals). Bars indicate median and quartiles (top and bottom, respectively). P values were calculated using Wilcoxon's test. Analysis for RBP3 concentration and ratio of RBP3 to VEGF were performed with Kruskal-Wallis test. When overall omnibus tests were significant ($P < 0.05$), Mann-Whitney U tests were used to determine the location of any significant pairwise differences.

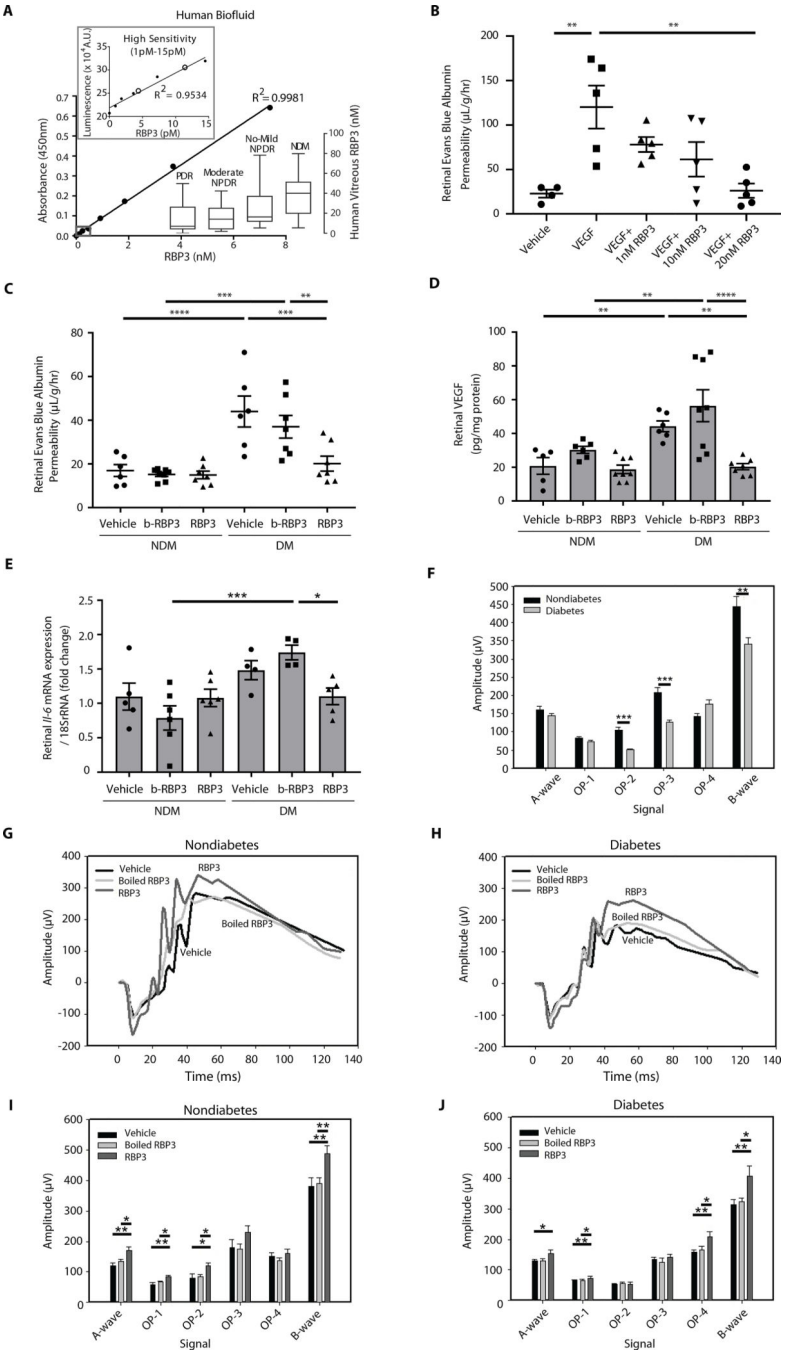

Fig. 2. Assessment of RBP3 concentrations in human biofluid and effects of intravitreal injection with hRBP3 peptide on DR in rats.

(**A**) RBP3 ELISA for vitreous and serum concentrations of RBP3 in individuals. Colorimetric ELISA for vitreous RBP3 concentration and luminescent ELISA (high sensitivity) for serum RBP3 concentration. Black circles are serum RBP3 concentration from individuals with NDM. A.U., arbitrary units. (**B**) Effects of recombinant hRBP3 (rhRBP3) on VEGF-mediated retinal vascular permeability (RVP) in rat (n = 4 to 5). (**C** to **E**) Effects of IVT injected rhRBP3 (20 nM) on (C) RVP, (D) VEGF protein expression, and

(E) *Il-6* mRNA expression in DM retina (n = 4 to 8). rRNA, ribosomal RNA. (**F** to **J**) Electroretinogram (ERG) at (F) baseline; NDM (n = 21), DM (n = 35), and (G to J) 3 days after IVT injection (n = 9 to 14). n = numbers of eyes. b-RBP3, boiled RBP3. All data are represented as means ± SEM. Group comparison was performed by analysis of variance (ANOVA). When overall F tests were significant ($P < 0.05$), Fisher's least significant difference test was used to determine the location of any significant pairwise differences.

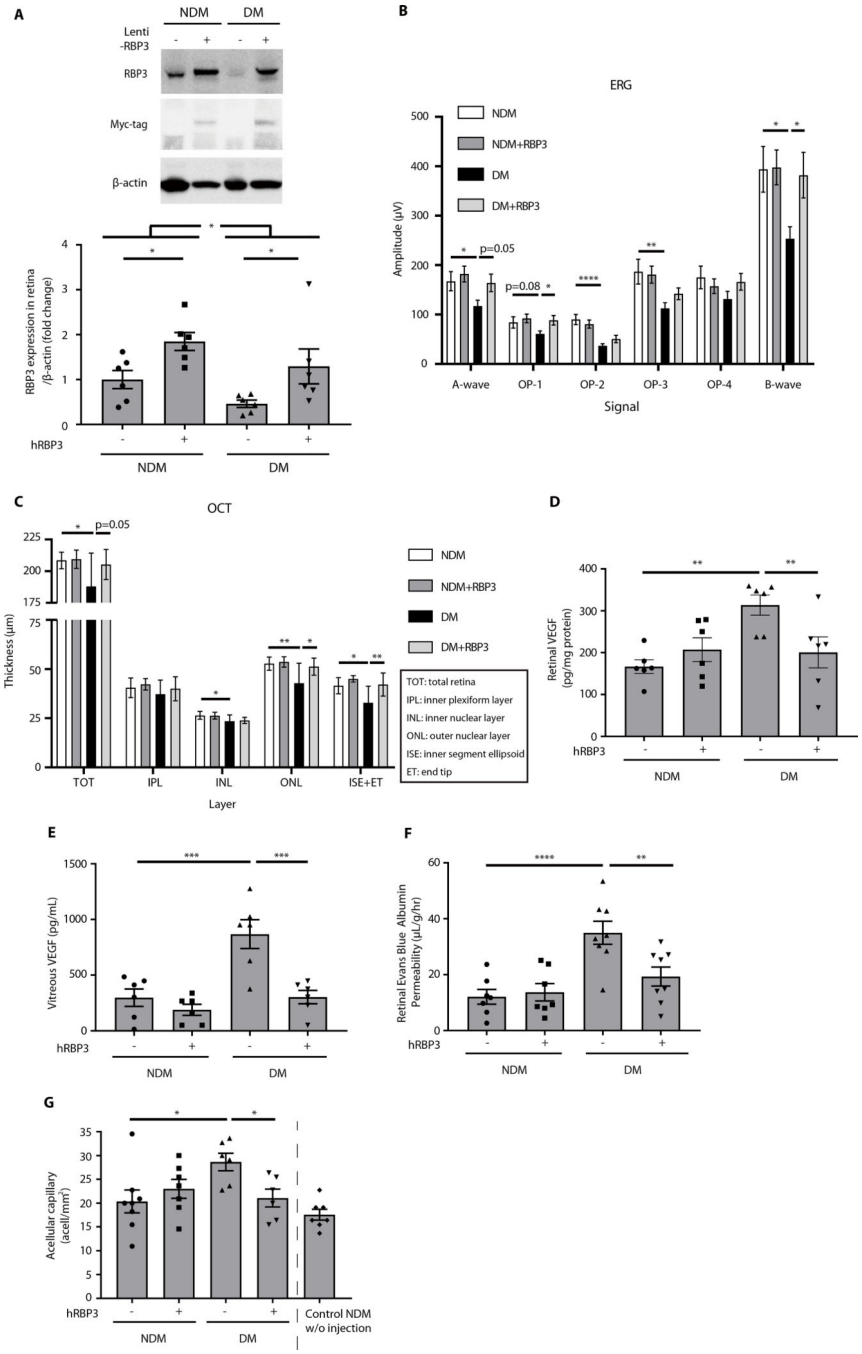

Fig. 3. Protective effects of lentiviral-mediated subretinal overexpression of hRBP3 on DR in rats.

(**A**) The expressions of endogenous RBP3 and exogenous RBP3 tagged with Myc in retina by immunoblot ($n = 6$), (**B**) ERG ($n = 10$ to 11), (**C**) OCT ($n = 6$ to 7), (**D** and **E**) VEGF expression in retina and vitreous ($n = 6$), and (**F**) RVP ($n = 7$ to 8) of DM rats for 2 months. (**G**) Quantification of acellular capillaries in retinal vascular pathology of DM rats for 6 months ($n = 6$ to 8). hRBP3^{-}, eye injected with luciferase gene only; hRBP3^{+}, eye injected

with hRBP3 and luciferase genes. *n* = numbers of eyes. All data are represented as means ± SEM. Group comparison was performed by ANOVA (same as Fig. 2).

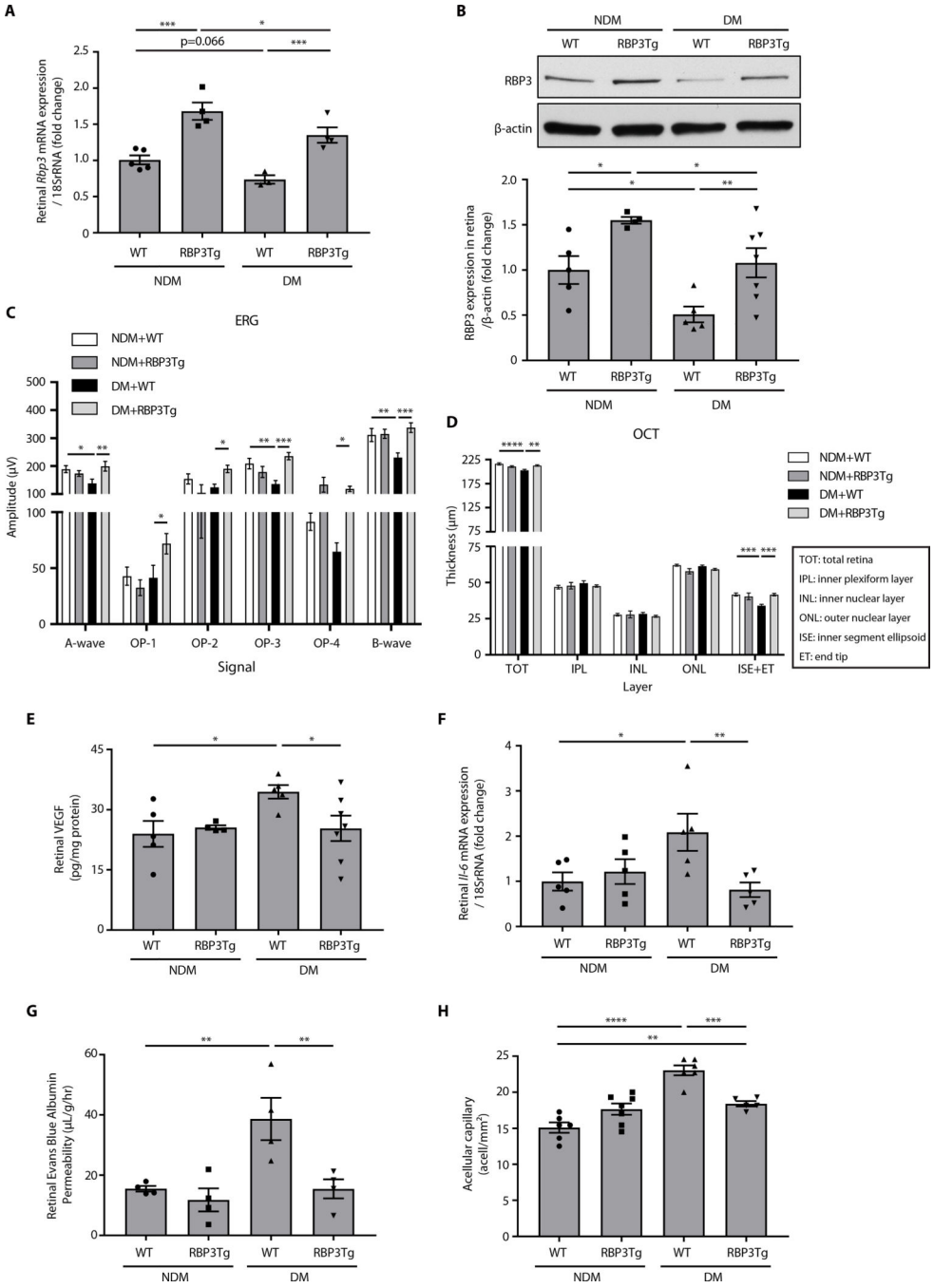

Fig. 4. Protective effects of hRBP3 on DR in RBP3 Tg mice with specific overexpression in the retina.

(**A**) *Rbp3* mRNA expressions (n = 3 to 5), (**B**) RBP3 protein expressions by immunoblot (n = 4 to 7), (**C**) ERG (n = 7 to 8), (**D**) OCT (n = 6 to 8), (**E**) VEGF protein expression (n = 4 to 7), (**F**) *Il-6* mRNA expression (n = 5), and (**G**) RVP (n = 4) in the retina of DM mice for 2 months. (**H**) Quantification of acellular capillaries in retina of DM mice for 6 months (n = 5 to 7). n = numbers of eyes. All data are represented as means ± SEM. Group comparison was performed by ANOVA (same as Figs. 2 and 3).

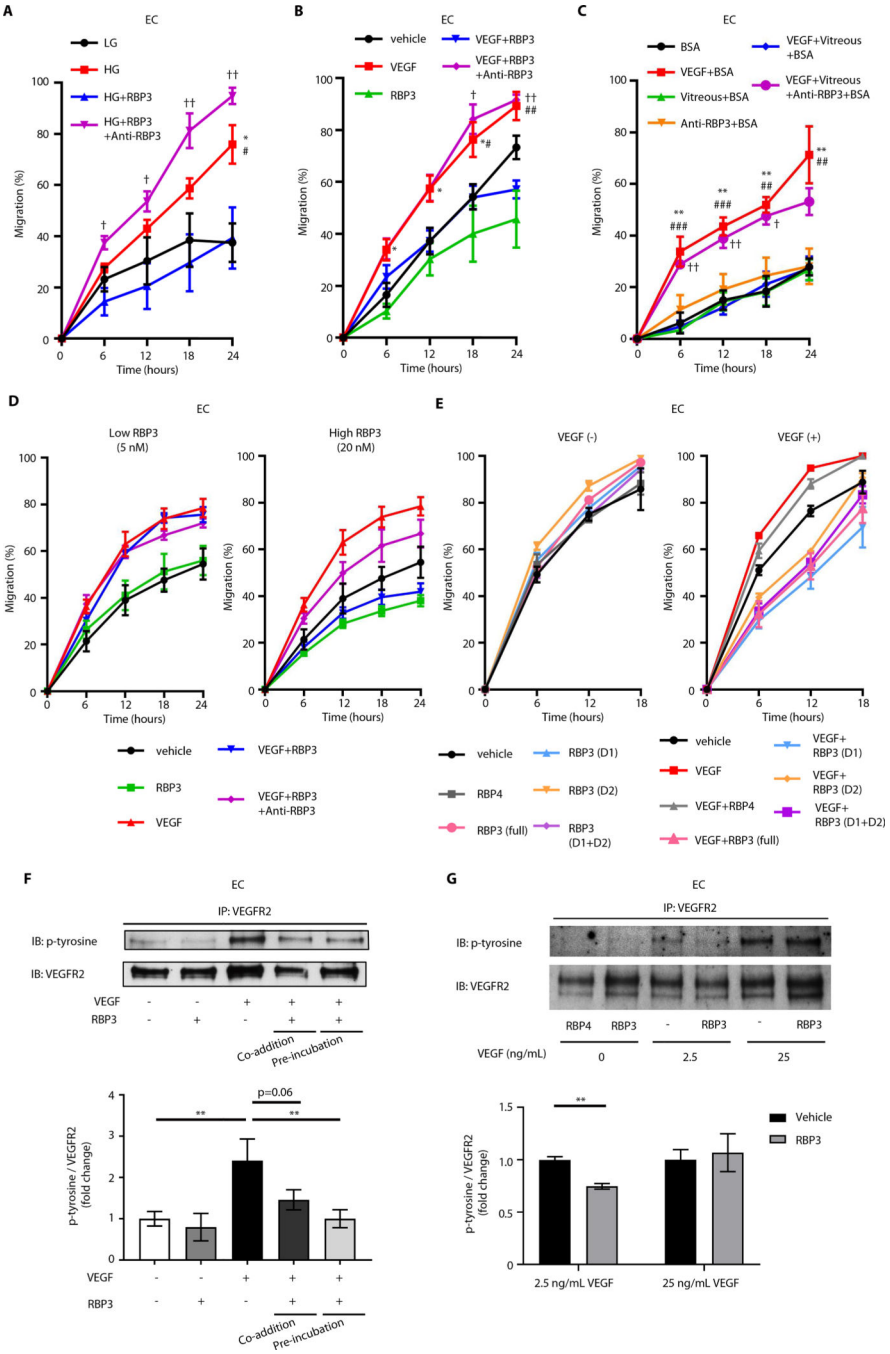

Fig. 5. Characterization of rhRBP3 on retinal vascular cells and Müller cells.

(**A** to **C**) Effects of rhRBP3 (0.25 μg/ml, 2 nM) or Medalist patient vitreous from protected eyes on 25 mM HG or rhVEGF (2.5 ng/ml)–induced endothelial migration in BRECs. (A) **P* < 0.05, LG versus HG; #*P* < 0.05, HG versus HG + rhRBP3; †*P* < 0.05, ††*P* < 0.01 HG + rhRBP3 versus HG + rhRBP3 + anti-RBP3. *n* = 4. (B) **P* < 0.05, vehicle versus rhVEGF; #*P* < 0.05, ##*P* < 0.01 VEGF versus VEGF + rhRBP3; †*P* < 0.05, ††*P* < 0.01 VEGF + rhRBP3 versus VEGF + rhRBP3 + anti-RBP3. *n* = 4 to 5. (C) ***P* < 0.01, bovine serum albumin (BSA) versus rhVEGF + BSA; ##*P* < 0.01, ###*P* < 0.001 rhVEGF + BSA versus

rhVEGF + vitreous + BSA; †$P < 0.05$, ††$P < 0.01$ VEGF + vitreous + BSA versus VEGF + vitreous + anti-RBP3 + BSA. $n = 3$. (**D**) Effects of rhRBP3 (5 or 20 nM) on rhVEGF (2.5 ng/ml)–induced endothelial migration in BRECs ($n = 4$). (**E**) Effects of different peptide of rhRBP3 (20 nM) on rhVEGF (2.5 ng/ml)–induced endothelial migration in bovine aortic endothelial cell ($n = 4$). (**F**) Tyrosine phosphorylation of VEGFR2 (pTyr-VEG-FR2) under rhRBP3 (0.25 μg/ml) and rhVEGF (2.5 ng/ml) stimulation in BRECs ($n = 3$). (**G**) pTyr-VEGFR2 under rhRBP4 (20 nM) or rhRBP3 (2.5 μg/ml, 20 nM) and rhVEGF stimulation with cross-linking assay by 3,3′-dithiobis(sulfosuccinimidyl propionate) (DTSSP) in BRECs ($n = 3$). P-tyrosine, tyrosine phosphorylation. All data are represented as means ± SEM. Group comparison was performed by ANOVA (same as Figs. 2 to 4).

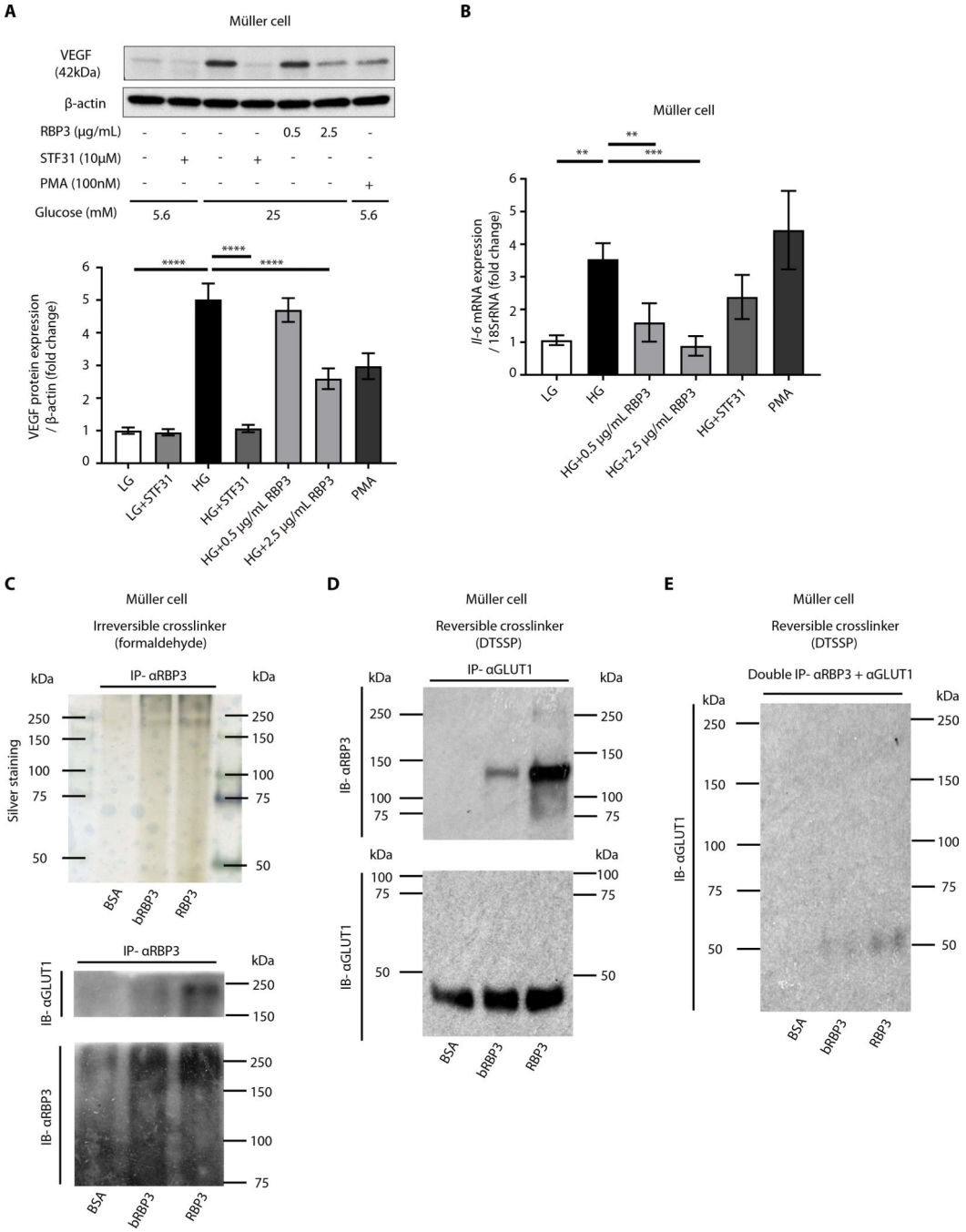

Fig. 6. Characterization of rhRBP3 on Müller cells.

(**A** and **B**) Effects of rhRBP3 on HG-induced VEGF protein expression ($n = 8$) and *Il-6* mRNA expression ($n = 6$). PMA, phorbol 12-myristate 13-acetate. (**C**) Cross-linking assay with formaldehyde. Silver staining and immunoblot. (**D** and **E**) Cross-linking assay with DTSSP. All data are represented as means ± SEM. Group comparison was performed by ANOVA (same as Figs. 2 to 5).

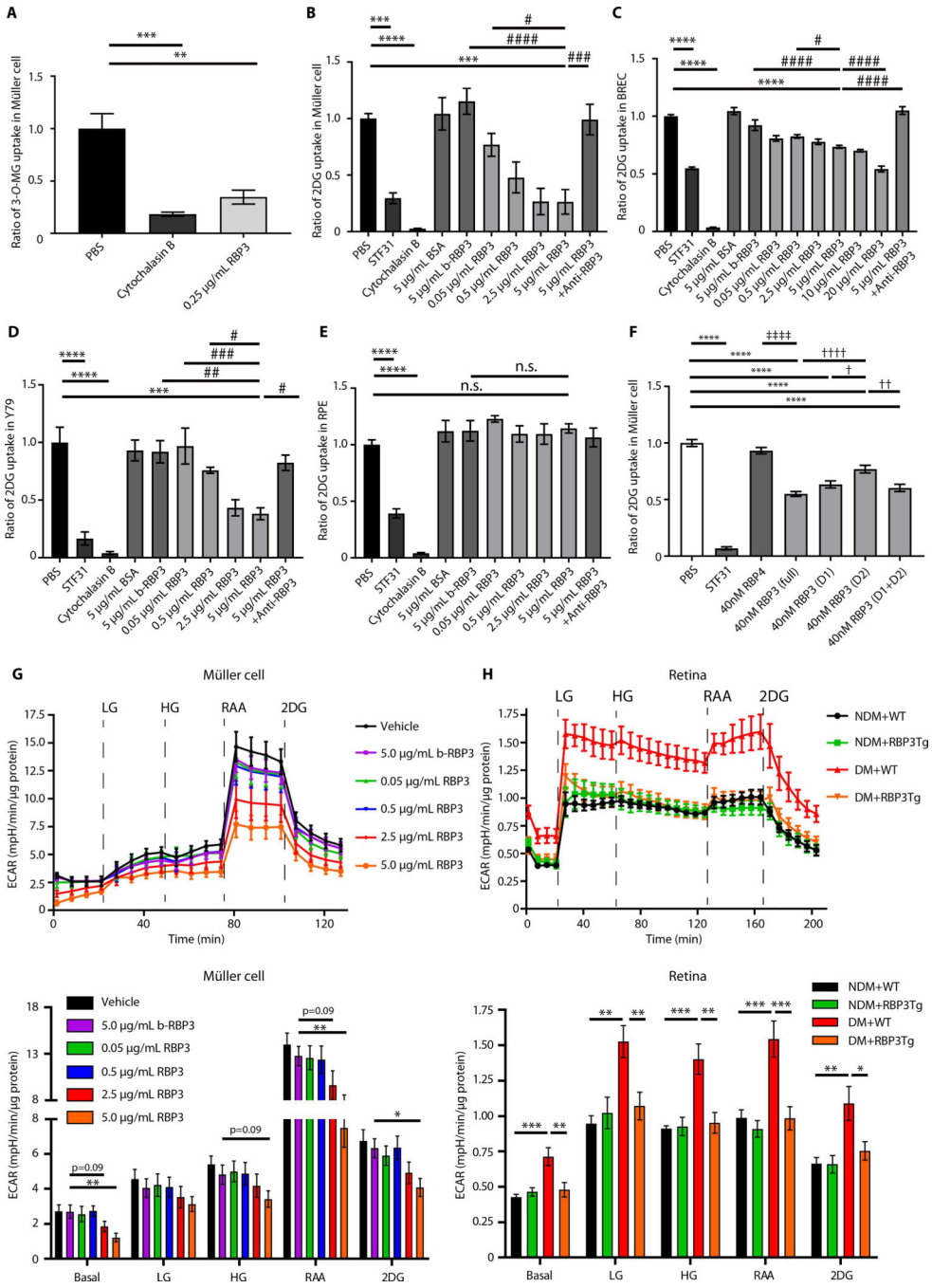

Fig. 7. Effects of rhRBP3 on glucose uptake and glycolytic flux in vitro and ex vivo.

(**A**) Effects of rhRBP3 on 3-*O*-MG uptake into Muller cells ($n = 3$). (**B** to **E**) Effects of rhRBP3 on 2DG uptake. (B) Müller cells ($n = 3$ to 6). (C) BRECs ($n = 3$ to 10). (D) Y79 cells ($n = 3$). (E) RPE cells ($n = 4$). (**F**) Effects of different size of rhRBP3 peptide on 2DG uptake ($n = 6$). Full, D1 and D2: full length, D1 and D2 of rhRBP3. (**G**) Extracellular acidification rate (ECAR) in Muller cells. LG, 5.6 mM glucose; HG, 25 mM glucose. Rotenone/antimycin A (RAA; 0.5 μM) and 2DG (50 mM) ($n = 8$). (**H**) ECAR in isolated retinas of all mice group of NDM or DM. RAA, 2.0 μM; 2DG, 100 mM. Number of retinas

evaluated: $n = 4$. All data are represented as means ± SEM. Group comparison was performed by ANOVA (same as Figs. 2 to 6). (A to F) $^{**}P < 0.01$, $^{***}P < 0.001$, and $^{****}P < 0.0001$, versus PBS; $^{\#}P < 0.05$, $^{\#\#}P < 0.01$, $^{\#\#\#}P < 0.001$, and $^{\#\#\#\#}P < 0.0001$, versus RBP3 (5 μg/ml); $^{\dagger}P < 0.05$, $^{\dagger\dagger}P < 0.01$, and $^{\dagger\dagger\dagger\dagger}P < 0.0001$, versus 40 nM RBP3 (D2); $^{\ddagger\ddagger\ddagger\ddagger}P < 0.0001$, 40 nM RBP4 versus 40 nM RBP3 (full). (G) $^{*}P < 0.05$, $^{**}P < 0.01$, b-RBP3 (5.0 μg/ml) versus RBP3 (5.0 μg/ml). (H) $^{*}P < 0.05$, $^{**}P < 0.01$, $^{***}P < 0.001$, versus DM + WT. n.s., not significant.